

# Multi-Responsive Nanogels for Targeted Anti-Cancer Drug Delivery

*Qiang Zhang,<sup>†</sup> Juan Colazo,<sup>‡</sup> Darren Berg,<sup>||</sup> Samuel M. Mugo<sup>||\*</sup> and Michael J. Serpe<sup>‡\*</sup>*

<sup>†</sup> Prof. Q. Zhang,

Current address: State Key Laboratory of Electroanalytical Chemistry, Changchun Institute of Applied Chemistry, Chinese Academy of Sciences, 5625 Renmin Street, Changchun 130022 (P.R. China)

<sup>‡</sup>J. Colazo, Prof. M. J. Serpe,

Department of Chemistry, University of Alberta, Edmonton, Alberta, T6G 2G2 Canada

E-mail: michael.serpe@ualberta.ca

<sup>||</sup> D. Berg, Prof. S. M. Mugo

Physical Sciences Department, MacEwan University, Edmonton, AB, T5J 4S2 Canada

E-mail: mugos@macewan.ca

**KEYWORDS:** *Nanogels, Drug delivery, Stimuli-responsive polymers, Biomolecular coatings*

**ABSTRACT.** Nanogels with a biomolecular coating (biocoating) were shown to be capable of triggered delivering anti-cancer drug Doxorubicin. The biocoating was formed utilizing binding between glycogen and the tetra-functional lectin Concanavalin A, which can be triggered to disassemble (and release) upon exposure to glucose and changes in solution pH. We also show the nanogel's thermoresponsivity can be used to accelerate Doxorubicin release. Moreover, we showed that transferrin immobilized on the nanogel surface could accelerate nanogel uptake by cancer cells. In these experiments, we showed that Doxorubicin was able to be released to the nucleus of human liver cancer cell line (HepG2) within 3 h. Doxorubicin loaded nanogels exhibit a strong growth inhibition ability toward HepG2. This investigation showcases how nanogel design and chemistry can be tuned to achieve useful biomedical applications.

## **1. INTRODUCTION**

Cancer remains a leading cause of mortality worldwide, accounting for approximately 8.2 million deaths in 2012.<sup>1</sup> According to statistics reported by the World Health Organization (WHO), global annual cancer cases are expected to rise from 14 million in 2012 to 22 million within the next two decades.<sup>1</sup> Although various therapies have been developed for cancer treatment, chemotherapy remains the most commonly used approach. Anti-cancer drugs are often utilized to treat recurrent cancers, but have several drawbacks, including poor water solubility, severe toxicity to normal cells, and inadequate drug concentrations at tumor sites.<sup>2</sup> Conventional chemotherapy is highly non-specific in targeting cancer cells, causing undesirable side effects to the patient, e.g., pain, hair loss, blood disorders, and negative effects on the nervous system.

Nanotechnology has been used to combat some of these issues, and to improve cancer treatment efficacy.<sup>3</sup> In recent years, a variety of nanoparticles have been used for drug delivery applications, including liposomes,<sup>4</sup> magnetic nanoparticles,<sup>5</sup> micelles,<sup>6</sup> gold nanoparticles,<sup>7</sup> silicone nanoparticles,<sup>8</sup> synthetic and natural polymers,<sup>9</sup> and carbon nanotubes.<sup>10</sup> Compared to traditional chemotherapeutics, nanoparticle-based platforms can improve solubility of poorly soluble drugs by encapsulating them in a hydrophilic compartment. Moreover, nanoparticles can protect the drugs from harsh environments found in the body, such as the low pH environment in the stomach and the presence of enzymes, which can degrade the drugs. For instance, nanocarriers have been shown to protect therapeutic RNA from nucleases in order to increase the lifetime and efficacy of genetic treatment systems.<sup>11</sup> These benefits combined lead to an improvement in drug lifetime and an extended plasma half-life of the drug in systemic circulation.<sup>12</sup>

Of particular interest for the submission here are hydrogel-based nanoparticles (nanogels), which are extremely porous materials capable of the loading and release of small molecules, including anti-cancer drugs, for targeted drug delivery applications. Nanogels can be tailored to be responsive to a variety of stimuli (pH, temperature, chemical and biological species) by integration of functional monomers or nanoparticles into their structure.<sup>13</sup> Our group's research is focused on the development of novel stimuli-responsive microgels/nanogels for use as sensors, artificial muscles, and drug delivery platforms.<sup>14</sup> In this submission, we report on stimuli-responsive nanogels with a biomolecular coating (biocoating) that can be used for targeted anti-cancer drug delivery (Figure 1).

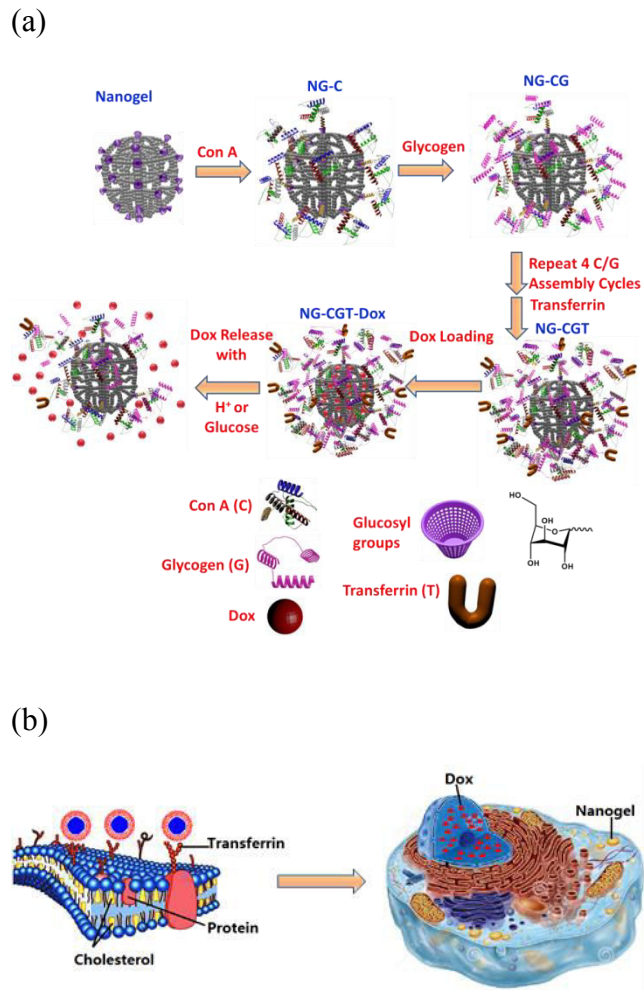


**Figure 1.** (a) Schematic illustration of biocoating generation, and Dox loading/release process, and (b) The targeting/delivery process.

## 2. RESULTS AND DISCUSSION

Glucosyl-functionalized nanogels were synthesized using free radical precipitation polymerization of N-isopropylacrylamide (pNIPAm, 90%), N,N'-methylenebis (acrylamide) (BIS, 5%), and glycosyloxyethyl methacrylate (GEM, 5%). The synthetic details for nanogel generation can be seen in Electronic Supporting Information (ESI). Then, Concanavalin A (Con A) was attached to the nanogel surface via its interaction with the glucosyl groups of GEM. Subsequently, glycogen was exposed to the nanogels, which attached to the Con A via sugar–

lectin-based biorecognition.<sup>15</sup> After 4 cycles of Con A and glycogen exposure, transferrin was added onto the biocoating through a similar glycoprotein–lectin binding mechanism — these nanogels are noted as NG-CGT. It has been reported that Con A contains 4 (tetramer) lectins at pH 7-8, which transitions to a state with 2 (dimer) lectins per molecule when solution pH decreases from 7.0 to 5.<sup>16</sup> For the system here, the transition of Con A from a tetramer to dimer results in a partial decrease in the density of the biocoating due to the lower degree of interactions between the dimeric Con A and glycogen.

It has been shown that transferrin receptors are upregulated by various cancer cells and overexpressed in various cancer cells in comparison to healthy cells.<sup>17</sup> Therefore, the transferrin localized on the outer surface of the biocoating can be used to specifically bind the nanogels to specific cancer cells (Figure 1b) where they can be endocytosed. We propose that the acidic conditions found in endosomes (pH = 4.5–6.0),<sup>18a</sup> will result in the breakdown of the biocoating, and release of the loaded drugs from endocytosed nanogels. Additionally, we hypothesize that glucose will be able to trigger the degradation of the biocoating through its competitive binding with glycogen for Con A. Finally, we hypothesize that temperature could be used to trigger drug release from the nanogels. Since pNIPAm-based nanogels collapse at solution temperature above ~32 °C,<sup>13c</sup> we hypothesize that the deswelling process of nanogels could force the drug out of the nanogels.

To begin, nanogels were synthesized, and their diameter measured using dynamic light scattering (DLS). As can be seen in the results in ESI, the nanogels exhibited a hydrodynamic radius (Rh) of 150 nm at 37 °C. After modification of the nanogels with the Con A–glycogen–transferrin coating, the diameter of nanogels increased to 180 nm at 37 °C. Figure 2a shows transmission electron microscope (TEM) images of the nanogels without the biocoating, which

reveals that the nanogels have a fairly uniform diameter of  $\sim 130$  nm ( $\pm 10$  nm). After coating Con A–glycogen–transferrin on the nanogel surface, diameters of nanogels increased from 130 nm ( $\pm 10$  nm) to 160 nm ( $\pm 15$  nm), as shown in Figure 2b. It has been reported that nanoparticles with a diameter of less than 200 nm can penetrate cellular membranes and incrementally accumulate in tumor tissues after cellular uptake.<sup>18b</sup> Therefore, these nanogels should be appropriate candidates for cellular level drug delivery. The assembly process of Con A–glycogen–transferrin was also monitored using quartz crystal microbalance (QCM) measurements, and the results are shown in Figure 2c. To conduct these measurements, a single layer of nanogels was deposited on the gold surface of the QCM crystal. Then, solutions of Con A ( $2$  mg mL<sup>-1</sup>) and glycogen ( $2$  mg mL<sup>-1</sup>) were alternatively flowed over the surface sequentially, four times. Finally, the outer transferrin layer was deposited on Con A-glycogen film by exposure of the surface to a transferrin solution ( $2$  mg mL<sup>-1</sup>) for 30 min. A decrease in the frequency was observed during the self-assembly process, which indicated the successful formation of a Con A/glycogen/transferrin coating on the nanogels.

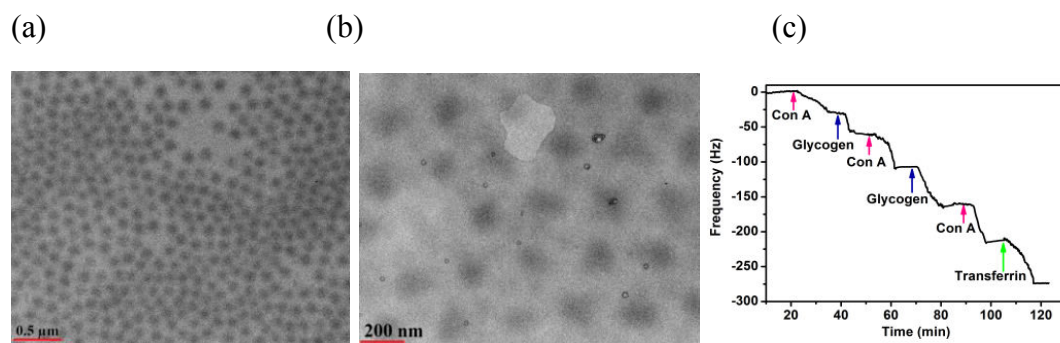


**Figure 2.** (a) TEM image of NG; (b) TEM image of NG-CGT; (c) QCM results for self-assembly of the Con A-Glycogen-Transferrin multilayers.

Doxorubicin (Dox) is a commonly used chemotherapeutic agent that has been effective in treating a variety of cancers, including hematological malignancies (blood cancers, like leukaemia and lymphoma), many types of carcinoma (solid tumors) and soft tissue sarcomas.<sup>19</sup>

Dox was used as a model drug in this investigation, and was loaded into the nanogels by incubating NG-CGT (10 mg) in a 2 mL Dox solution ( $4 \text{ mg mL}^{-1}$ , pH 7.4) for 24 h. After Dox loading, the nanogels were rinsed by centrifugation (4 times) using excess Tris-HCl buffer solution (pH 7.4), and no leakage of Dox from nanogels was observed visually. Meanwhile, the color of nanogels changed from white to red due to the loading of Dox. We propose that Dox slowly diffuses through the Con A-glycogen coating due to the significant Dox concentration difference between the Dox solution and the inside of the nanogels. While this is the case, we propose that the biocoating can effectively block Dox from leaking out of the nanogels due to the spatial obstruction formed at the surface from the of Con A-glycogen coating. For comparison, uncoated nanogels were also loaded with Dox, and were soaked in Tris-HCl buffer solution. In this case, significant leakage of Dox from nanogels was observed.

Next, we investigated the kinetics of Dox release from NG-CGT in response to solution pH, temperature, and exposure to glucose. The results are shown in Figure 3. For these experiments, nanogels were dispersed in a buffer solution at a concentration of  $0.1 \text{ mg mL}^{-1}$  and triggered to release by exposure to the stimuli specified above. At specific times, samples were collected and the nanogels were removed from the solution via centrifugation, and emission spectra were measured in the range of 520 – 800 nm at 465 nm excitation (ESI). The concentration of Dox was determined according to emission intensity at 580 nm using a calibration curve (ESI).

Firstly, pH triggered Dox release was measured over the pH range of 4-7.4. At neutral pH (7.4, similar to normal physiological conditions), we determined that 1.8 ppm of drug was released after 20 h, while 2.1 ppm was released after 2 days. When the solution pH decreased to 4, the release rate dramatically increased, and 7.2 ppm Dox was released after 20 h incubation, while 6.5 ppm was released at pH 5 in the same test condition. It has been reported that Dox is

able to kill cells at a concentration of 5 ppm, therefore these concentrations are therapeutically relevant.<sup>20</sup> For these nanogels, the Dox release was attributed to the degradation of the biocoating at low pH, which we propose opens up pores for the Dox release. Again, this behavior is significant because of the acidic conditions found in endosomes.<sup>18</sup> Next, we evaluated the ability of Dox to be released from the nanogels in response to glucose exposure. It has been reported that Con A can bind to glucose through multiple hydrogen bonding interactions.<sup>21</sup> In this case, we hypothesize that the biocoating will become more porous in the presence of glucose and Dox will be released. The resultant release profiles are shown in Figure 3b, and it can be seen that as the glucose concentration increased from 400 ppm to 1200 ppm, the amount of Dox released also increased from 1.8 ppm to 7.6 ppm. Lastly, Dox release in response to temperature was also determined, and the results can be seen in Figure 3c. The NG-CGT exhibited a lower critical solution temperature (LCST) of 36 °C measured using DLS (Figure 3d), which is much higher than that of pure pNIPAm (32 °C). We attributed this to the presence of hydrophilic glucosyl groups in the NG-CGT. The ability of functional group polarity to alter the LCST of pNIPAm is a well-known phenomenon.<sup>22</sup> The LCST of NG-CGT makes them an ideal candidate for drug delivery because of its proximity to body temperature. Furthermore, NG-CGT exhibit more significant changes in volume and size over micelles, liposomes, and other related nanoparticles when local body temperature undergoes small changes, which makes it possible to tune the drug release rate by controlling the local body temperature.

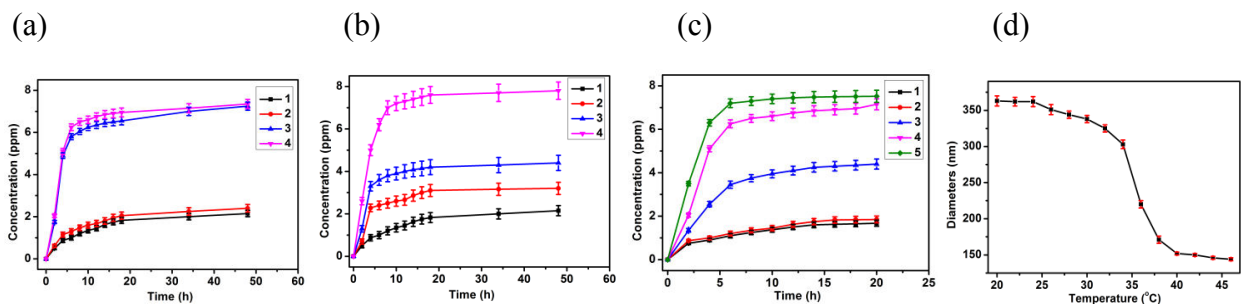


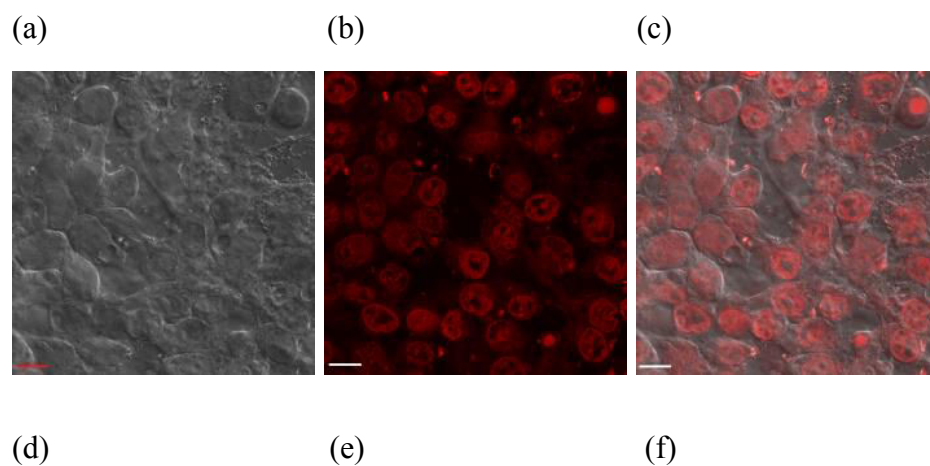


**Figure 3.** In vitro drug release profiles of free Dox: (a) triggered by pH (1: pH 7.4, 2: pH 6, 3: pH 5, 4: pH 4); (b) triggered by glucose (1: 400 ppm, 2: 700 ppm, 3: 1000 ppm, 4: 1300 ppm) at pH 7.4; (c) triggered by temperature (1: pH 7.4 at 25 °C; 2: pH 7.4 at 37 °C; 3: pH 4 at 25 °C; 4: pH 4 at 37 °C; 5: pH 4 at 45 °C). (d) NG-CGT diameters as a function of temperature determined by DLS.

As can be seen in Figure 3c, when the solution temperature was increased from 25 °C to 37 °C at pH 7.4, no acceleration of the Dox release rate was observed, due to the fact that the biocoating was mainly intact. However, at pH 4, the same thermal treatment yielded a significant increase in the Dox release rate, which was due to the increased porosity of the biocoating. The partial degradation process of the Con-glycogen coating was monitored using QCM (ESI). As the NG-CGT was exposed to pH 5 or 1200 ppm glucose solution, the frequency of QCM dramatically increased, indicating substantial mass loss of the biofilm (ESI). In order to investigate stability of the drug delivery system over long time, Dox loaded NG-CGT was freeze-dried and stored at -20 °C for two months. These nanogels exhibited similar pH triggered Dox release behavior compared to the initial nanogels (ESI).

The human liver cancer cell line (HepG2) was used to investigate the targeting ability and Dox release of NG-CGT. The study was conducted by incubating the HepG2 cells in Dox loaded NG-CGT solution (0.05 mg mL<sup>-1</sup>) for 3 h. As can be in Figure 4b, the HepG2 cells exhibited very strong fluorescence after the incubation, although native HepG2 cells do not exhibit such fluorescence (ESI). Based on this fact, the delivery of Dox to the cells could be confirmed. Furthermore, fluorescence intensity could be related to the amount of Dox in the cells. When HepG2 cells were exposed to 0.025mg mL<sup>-1</sup> Dox loaded NG-CGT, the cells exhibited less fluorescence (ESI). [Through comparison of optical and fluorescence images of HepG2, it appears that most of Dox gathered at the cell nucleus, as shown in Figure 4a-c. While this appears to be the case, more experiments will need to be conducted to confirm.](#) It has been

reported that Dox reduces division and growth of cancer cells by inhibiting DNA replication and RNA synthesis through intercalation into DNA.<sup>23</sup> In this investigation, we noted an inhibition of growth of HepG2 cells in the presence of 0.05 mg mL<sup>-1</sup> Dox. Our work confirms that NG-CGT is an efficient material for anti-cancer drug delivery. In order to investigate the targeting function of transferrin, nanogels without transferrin (NG-CG) was also used to deliver Dox into cells. All of the experiments and microscopy tests were conducted at the same conditions of the NG-CGT experiments, and the results were shown in Figure 4 (d-f). HepG2 exhibited much weaker fluorescence intensity compared with that treated using Dox loading NG-CG, which indicated that the transferrin played a critical role in accelerating the uptake of nanogels by HepG2. The transferrin has very high affinity for the transferrin receptor (a type II transmembrane glycoprotein) on the surface of HepG2. Once binding the transferrin receptor, the NG-CGT/transferrin receptor complex was internalized in clathrin-coated pits through receptor-mediated endocytosis.<sup>24</sup>



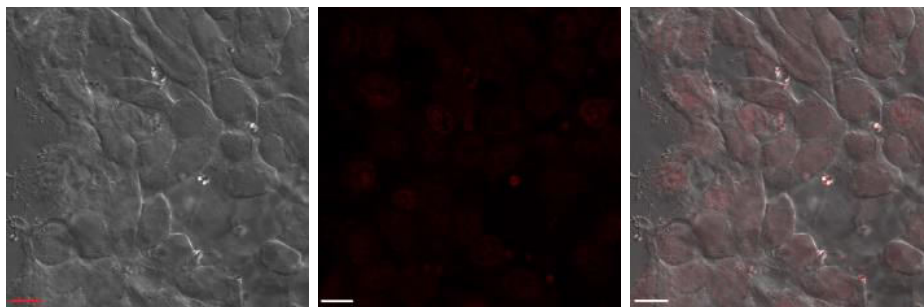


**Figure 4.** (a-c) Microscopy images of HepG2 cells incubated in  $0.05 \text{ mg mL}^{-1}$  NG-CGT Dox loaded solution. (a) Bright field microscopy image. (b) Fluorescence microscopy image; excitation at 488 nm. (c) Converged image of bright field and fluorescence microscopy images. (d-f) Microscopy images of HepG2 cells incubated in NG-CG Dox loaded (without transferrin on the surface.) solution ( $0.05 \text{ mg mL}^{-1}$ ). (d) Bright field microscopy image. (e) Fluorescence microscopy image; excitation at 488 nm. (f) Converged image of bright field and fluorescence microscopy images. Scale bars in all images are  $20 \mu\text{m}$ .

### 3. Conclusion

In summary, we reported a drug delivery system that was prepared by layer-by-layer self-assembly of Con A, glycogen, and transferrin on glucosyl functionalized nanogels. The release of drug from nanogels could be triggered by changing pH, glucose, and temperature.  $\text{H}^+$  and glucose generate substantial porosity in biocoating, which lead release of drug from nanogels. Temperature also exhibits tremendous effect on release rate due to thermal responsibility of pNIPAm. HepG2 was used to investigate anti-cancer drug delivery capability of nanogels. The drug was successfully delivered into the nucleuses of HepG2, which prevent growth of cancer cells by mitigating DNA duplication. The cell experiment demonstrated that the transferrin played a key role in accelerating cytotoxic agents' endocytosis of cancer cells. This investigation

demonstrates the functional chemistry diversity and versatility of pNIPAm-based nanogel manipulation to achieve complex responsivities valuable for drug delivery applications.

## **ASSOCIATED CONTENT**

### **Supporting Information.**

The following files are available free of charge.

Materials; Measurement; Synthesis of nanogels; Nanogel diameters at 30 °C determined by DLS; QCM results for the disassembly of biocoating in response to glucose and pH; Calibration curve of fluorescence intensity at 580 nm as a function of Dox concentration; In vitro drug release profiles of free Dox triggered by pH; Fluorescence microscopy images of HepG2 cells.

## **AUTHOR INFORMATION**

### **Corresponding Author**

michael.serpe@ualberta.ca; mugos@macewan.ca

## **ACKNOWLEDGMENT**

MJS acknowledges funding from the University of Alberta (the Department of Chemistry and the Faculty of Science), the Natural Sciences and Engineering Research Council of Canada (NSERC), the Canada Foundation for Innovation (CFI), the Alberta Advanced Education & Technology Small Equipment Grants Program (AET/SEGP), Grand Challenges Canada and IC-IMPACTS. Q. Z. acknowledges financial support through an Alberta Innovates Technology Futures (AITF) Postdoctoral Fellowship. Q. Z. also acknowledges support from the National Science Foundation of China (No: 21604091). SMM acknowledges MacEwan Research for Funding.

## REFERENCES

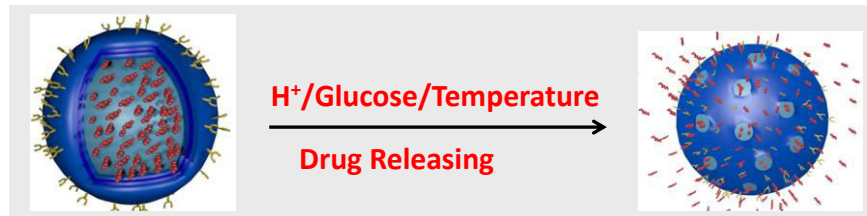
1. McGuire, S. World Cancer Report 2014. Geneva, Switzerland: World Health Organization, International Agency for Research on Cancer, WHO Press, 2015. *Adv. Nutri.* **2016**, *7*, 418-419.
2. Luo, Y.; Prestwich, G. Cancer-targeted polymeric drugs. *Curr. Cancer Drug Targets*, **2002**, *2*, 209-226.
3. Sun, T.; Zhang, Y. S.; Pang, B.; Hyun, D. C.; Yang, M.; Xia, Y. Engineered Nanoparticles for Drug Delivery in Cancer Therapy. *Angew. Chem. Int. Ed.* **2014**, *53*, 12320-12364.
4. Jiang, L.; Li, L.; He, X.; Yi, Q.; He, B.; Cao, J.; Pan, W.; Gu, Z. Overcoming drug-resistant lung cancer by paclitaxel loaded dual-functional liposomes with mitochondria targeting and pH-response. *Biomaterials* **2015**, *52*, 126-139.
5. Yang, G.; Gong, H.; Liu, T.; Sun, X.; Cheng, L.; Liu, Z. Two-dimensional magnetic WS<sub>2</sub>@Fe<sub>3</sub>O<sub>4</sub> nanocomposite with mesoporous silica coating for drug delivery and imaging-guided therapy of cancer. *Biomaterials* **2015**, *60*, 62-71.
6. Yu, H.; Cui, Z.; Yu, P.; Guo, C.; Feng, B.; Jiang, T.; Wang, S.; Yin, Q.; Zhong, D.; Yang, X.; Zhang, Z.; Li, Y. pH- and NIR Light-Responsive Micelles with Hyperthermia-Triggered Tumor Penetration and Cytoplasm Drug Release to Reverse Doxorubicin Resistance in Breast Cancer. *Adv. Funct. Mater.* **2015**, *25*, 2489-2500.
7. Qiu, L.; Chen, T.; Oecsoy, I.; Yasun, E.; Wu, C.; Zhu, G.; You, M.; Han, D.; Jiang, J.; Yu, R.; Tan, W. A Cell-Targeted, Size-Photocontrollable, Nuclear-Uptake Nanodrug Delivery System for Drug-Resistant Cancer Therapy. *Nano Lett.* **2015**, *15*, 457-463.
8. Kong, F.; Zhang, X.; Zhang, H.; Qu, X.; Chen, D.; Servos, M.; Makila, E.; Salonen, J.; Santos, H. A.; Hai, M.; Weitz, D. A. Inhibition of Multidrug Resistance of Cancer Cells by Co-Delivery of DNA Nanostructures and Drugs Using Porous Silicon Nanoparticles@Giant Liposomes. *Adv. Funct. Mater.* **2015**, *25*, 3330-3340.
9. Satsangi, A.; Roy, S. S.; Satsangi, R. K.; Tolcher, A. W.; Vadlamudi, R. K.; Goins, B.; Ong, J. L. Synthesis of a novel, sequentially active-targeted drug delivery nanoplatfor for breast cancer therapy. *Biomaterials* **2015**, *59*, 88-101.
10. Shao, W.; Paul, A.; Zhao, B.; Lee, C.; Rodes, L.; Prakash, S. Carbon nanotube lipid drug approach for targeted delivery of a chemotherapy drug in a human breast cancer xenograft animal model. *Biomaterials* **2013**, *34*, 10109-10119.
11. (a) Parodi, A.; Corbo, C.; Cevenini, A.; Molinaro, R.; Palomba, R.; Pandolfi, L.; Agostini, M.; Salvatore, F.; Tasciotti, E. Enabling cytoplasmic delivery and organelle targeting by surface modification of nanocarriers. *Nanomedicine* **2015**, *10*, 1923-1940; (b) Wang, J.; Lu, Z.; Wientjes, M. G.; Au, J. L.-S., Delivery of siRNA therapeutics: barriers and carriers. *The AAPS journal* **2010**, *12*, 492-503.
12. (a) Cully, M. Drug delivery nanoparticles improve profile of molecularly targeted cancer drug. *Nat. Rev. Drug Discov.* **2016**, *15*, 231-231; (b) Wan, L.; Jiao, J.; Cui, Y.; Guo, J.; Han, N.; Di, D.; Chang, D.; Wang, P.; Jiang, T.; Wang, S. Hyaluronic acid modified mesoporous carbon nanoparticles for targeted drug delivery to CD44-overexpressing cancer cells. *Nanotechnology* **2016**, *27*, 135102-135113.
13. (a) Hellweg, T. Responsive core-shell microgels: Synthesis, characterization, and possible applications. *J. Polym. Sci. Pt. B-Polym. Phys.* **2013**, *51*, 1073-1083; (b) Zhang, Q. M.; Ahiabu, A.; Gao, Y.; Serpe, M. J., CO<sub>2</sub>-switchable poly (N-isopropylacrylamide) microgel-

- based etalons. *J. Mater. Chem. C* **2015**, *3*, 495-498; (c) Zhang, Q. M.; Li, X.; Islam, M. R.; Wei, M.; Serpe, M. J., Light switchable optical materials from azobenzene crosslinked poly (N-isopropylacrylamide)-based microgels. *J. Mater. Chem. C* **2014**, *2*, 6961-6965; (d) Molina, M.; Asadian-Birjand, M.; Balach, J.; Bergueiro, J.; Miceli, E.; Calderon, M., Stimuli-responsive nanogel composites and their application in nanomedicine. *Chem. Soc. Rev.* **2015**, *44*, 6161-6186; (e) Raemdonck, K.; Demeester, J.; De Smedt, S., Advanced nanogel engineering for drug delivery. *Soft Matter* **2009**, *5*, 707-715; (f) Lyon, L. A.; Meng, Z. Y.; Singh, N.; Sorrell, C. D.; John, A. S., Thermoresponsive microgel-based materials. *Chem. Soc. Rev.* **2009**, *38*, 865-874; (g) Saxena, S.; Hansen, C. E.; Lyon, L. A., Microgel Mechanics in Biomaterial Design. *Acc. Chem. Res.* **2014**, *47*, 2426-2434; (h) Seiffert, S., Small but Smart: Sensitive Microgel Capsules. *Angew. Chem. Int. Ed.* **2013**, *52*, 11462-11468.
14. (a) Zhang, Q. M.; Wang, W.; Su, Y.-Q.; Hensen, E. J.; Serpe, M. J., Biological Imaging and Sensing with Multiresponsive Microgels. *Chem. Mater.* **2015**, *28*, 259-265; (b) Zhang, Q. M.; Berg, D.; Mugo, S. M.; Serpe, M. J., Lipase-modified pH-responsive microgel-based optical device for triglyceride sensing. *Chem. Commun.* **2015**, *51*, 9726-9728; (c) Zhang, Q. M.; Xu, W.; Serpe, M. J., Optical Devices Constructed from Multiresponsive Microgels. *Angew. Chem. Int. Ed.* **2014**, *53*, 4827-4831; (d) Li, X.; Serpe, M. J., Understanding and Controlling the Self-Folding Behavior of Poly (N-Isopropylacrylamide) Microgel-Based Devices. *Adv. Funct. Mater.* **2014**, *24*, 4119-4126; (e) Islam, M. R.; Li, X.; Smyth, K.; Serpe, M. J., Polymer-Based Muscle Expansion and Contraction. *Angew. Chem. Int. Ed.* **2013**, *52*, 10330-10333; (f) Sorrell, C. D.; Serpe, M. J., Reflection Order Selectivity of Color-Tunable Poly (N-isopropylacrylamide) Microgel Based Etalons. *Adv. Mater.* **2011**, *23*, 4088-4092; (g) Sorrell, C. D.; Carter, M. C.; Serpe, M. J., Color Tunable Poly (N-Isopropylacrylamide)-co-Acrylic Acid Microgel–Au Hybrid Assemblies. *Adv. Funct. Mater.* **2011**, *21*, 425-433.
  15. Sato, K.; Kodama, D.; Anzai, J.-I. Electrochemical determination of sugars by use of multilayer thin films of ferrocene-appended glycogen and concanavalin A. *Anal. Bioanal. Chem.* **2006**, *386*, 1899-1904.
  16. Zhu, Y.; Tong, W.; Gao, C., Molecular-engineered polymeric microcapsules assembled from Concanavalin A and glycogen with specific responses to carbohydrates. *Soft Matter* **2011**, *7*, 5805-5815.
  17. (a) Dautry-Varsat, A.; Ciechanover, A. Lodish, H. F., pH and the recycling of transferrin during receptor-mediated endocytosis. *PNAS* **1983**, *80*, 2258-2262; (b) Ryschich, E.; Huszty, G.; Knaebel, H. P.; Hartel, M.; Buchler, M. W.; Schmidt, J., Transferrin receptor is a marker of malignant phenotype in human pancreatic cancer and in neuroendocrine carcinoma of the pancreas. *Eur. J. Cancer* **2004**, *40*, 1418-1422.
  18. (a) Murphy, R. F.; Powers, S.; Cantor, C. R. Endosome pH measured in single cells by dual fluorescence flow cytometry: rapid acidification of insulin to pH 6. *J. Cell Biol.* **1984**, *98*, 1757-1762; (b) Kim, K.; Kim, J. H.; Park, H.; Kim, Y.-S.; Park, K.; Nam, H.; Lee, S.; Park, J. H.; Park, R.-W.; Kim, I.-S.; Choi, K.; Kim, S. Y.; Park, K.; Kwon, I. C., Tumor-homing multifunctional nanoparticles for cancer theragnosis: Simultaneous diagnosis, drug delivery, and therapeutic monitoring. *J. Controlled Release* **2010**, *146*, 219-227.
  19. Tacar, O.; Sriamornsak, P.; Dass, C. R., Doxorubicin: an update on anticancer molecular action, toxicity and novel drug delivery systems. *J. Pharm. Pharmacol.* **2013**, *65*, 157-170.

20. Eliaz, R. E.; Nir, S.; Marty, C.; Szoka, F. C., Determination and modeling of kinetics of cancer cell killing by doxorubicin and doxorubicin encapsulated in targeted liposomes. *Cancer Res.* **2004**, *64*, 711-718.
21. Goldstein, I.; Hollerman, C.; Smith, E. Protein-carbohydrate interaction. II. Inhibition studies on the interaction of concanavalina with polysaccharides. *Biochemistry* **1965**, *4*, 876-883.
22. Schild, H. Poly ( N-isopropylacrylamide): experiment, theory and application. *Prog. Polym. Sci.* **1992**, *17*, 163-249.
23. Li, H.; Cui, Y.; Sui, J.; Bian, S.; Sun, Y.; Liang, J.; Fan, Y.; Zhang, X., Efficient Delivery of DOX to Nuclei of Hepatic Carcinoma Cells in the Subcutaneous Tumor Model Using pH-Sensitive Pullulan–DOX Conjugates. *ACS Appl. Mater. Interfaces* **2015**, *7*, 15855-15865.
24. Daniels, T. R.; Delgado, T.; Helguera, G.; Penichet, M. L. The transferrin receptor part II: targeted delivery of therapeutic agents into cancer cells. *Clin. Immunol.* **2006**, *121*, 159-176.

## TOC

---



*Qiang Zhang, Juan Colazo, Darren Berg, Samuel M. Mugo and Michael J. Serpe*

**Multi-Responsive Nanogels for Targeting Anti-Cancer Drug Delivery**

The nanogels are capable of delivering anti-cancer drug to nucleus of human liver cancer cell line, which are triggered by change in glucose concentration, pH and temperature.

---